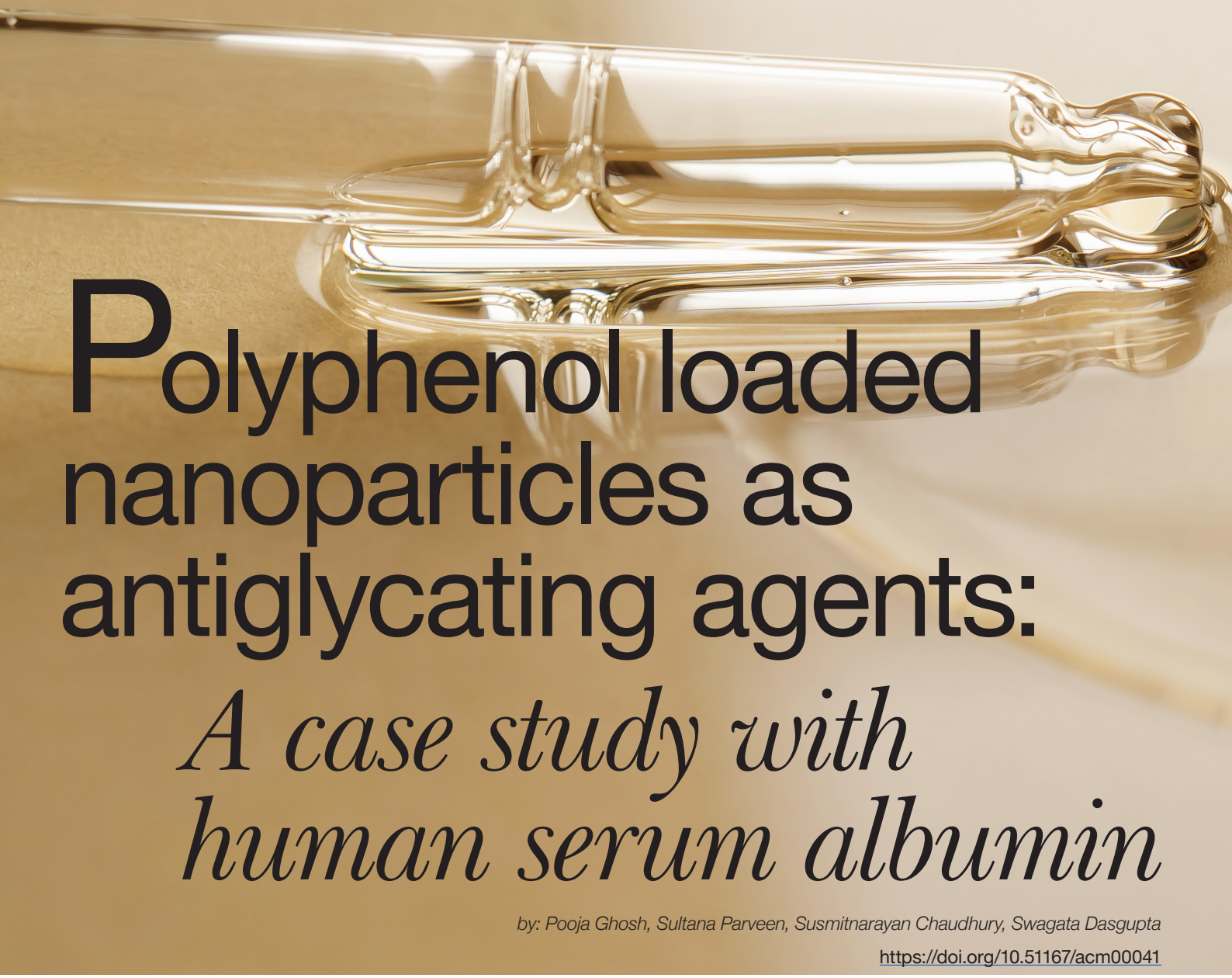

Polyphenol loaded nanoparticles as antiglycating agents: *A case study with human serum albumin*

by: Pooja Ghosh, Sultana Parveen, Susmitnarayan Chaudhury, Swagata Dasgupta

https://doi.org/10.51167/acm00041

Advanced glycation end products (AGEs) formed through nonenzymatic glycation results in diseases including diabetic complications, Alzheimer's disease and atherosclerosis etc. The development of novel antiglycating agents has thus become an important area of research. In our present work, we have reported the inhibitory activity of morin loaded PLGA NPs (MPNPs) on the D-ribose induced glycation of human serum albumin (HSA) based on spectroscopic studies. MPNPs were characterized by spectroscopic and microscopic techniques. HSA was incubated with ribose at 37 °C for one month and the formation of AGEs was confirmed from fluorescence studies, the increase in absorbance and the measurement of free amino groups. Further HSA and ribose mixtures incubated with MPNPs showed significant reduction in the extent of advanced glycation end product formation that were confirmed by UV-Vis and fluorescence spectroscopy and matrix-assisted laser desorption/ionization time-of-flight (MALDI-ToF) techniques. The structural changes induced by MPNPs were further confirmed by circular dichroism studies. Our findings suggest that MPNPs have the potential to be used antiglycating agents.

Pooja Ghosh

Dr. Pooja Ghosh is a Research Associate in Prof. Priyadarsi De's group in the Department of Chemical Sciences at the Indian Institute of Science Education and Research Kolkata (IISER Kolkata), India since March, 2019. She received her Ph.D. in 2018 from the Indian Institute of Technology Kharagpur (IIT Kharagpur), India with Prof. Dasgupta. She has 25 peer-reviewed publications to her credit. Her major research interests are in the field of protein chemistry, biophysical chemistry, nanoparticles & drug delivery. Her current research interests include designing different polymeric architectures for potential applications in protein aggregation field.

Susmitnarayan Chaudhury

Dr. Susmitnarayan Chaudhury received his PhD in Chemistry from the Indian Institute of Technology, Kharagpur India under the guidance of Prof. Dasgupta. He is trained as a chemist with a keen interest in biological system. Susmit is currently working as a postdoctoral research associate in Karissa Sanbonmatsu's team at Los Alamos National Laboratory, USA. His research interests revolve around visualizing biomolecules (RNA) in action which provides an insight to the mechanism of a particular biological process.

Introduction

Protein glycation is a non-enzymatic reaction between carbonyl groups of reducing sugars and the free amino groups of proteins. It is also commonly known as the Maillard reaction or browning reaction and passes through early, intermediate and advanced stages. In the early stage, carbonyl groups of reducing sugars react with the free amino groups of proteins to form reversible unstable Schiff bases. The Schiff bases then undergo Amadori rearrangement which leads to the formation of intermediate products, termed as Amadori products.[1] The Amadori products undergo further oxidation, dehydration and fragmentation which cause the formation of reactive oxygen species (ROS) and reactive carbonyl compounds. As they continue to react with amino groups of proteins, they lead to the formation of brown, fluorescent, insoluble, irreversible and heterogeneous compounds known as advanced glycation end products (AGEs).[2,3] AGEs are considered to be a marker of several severe diseases such as arteriosclerosis, renal failure and neurodegenerative diseases including Alzheimer's disease and Parkinson's disease,[4-6] but they also increase during the normal aging[7-8] process. AGEs are generally formed in the body in excess during aging and diabetes mellitus, the latter usually caused by a high level of glucose.

Protein glycation generally occurs in presence of several reducing sugars. Glucose, galactose[9], sialic acid[10], mannose[11], glucose 6-phosphate[12], glyceraldehydes[13], and fructose[14] have been used ***in vitro*** as glycating

Sultana Parveen

Dr. Sultana Parveen received her Bachelor's and Master's degree in Chemistry from Jadavpur University under the guidance of Prof Suman Das. She received her doctoral degree in protein chemistry from Indian Institute of Technology, Kharagpur under the supervision of Prof Swagata Dasgupta. Her research area mainly focused on the characterization and applications of protein films obtained from discarded cataractous eye protein isolates.

Swagata Dasgupta

Dr. Swagata Dasgupta is a Professor in the Department of Chemistry at the Indian Institute of Technology Kharagpur (IIT Kharagpur), India. She received her Ph.D. degree from RPI USA. For the past 25 years, her research group at IIT Kharagpur has investigated different aspects of Protein Chemistry mainly protein-small molecule and protein-protein interactions in addition to protein fibrillation studies and protein-nanoparticle interactions. She has guided over 30 doctoral students and published more than 150 research articles. She serves on the Editorial Board of several journals and is an active member of many committees. She is also a Fellow of the Indian Academy of Sciences, Bangalore.

agents. Glucose has been commonly used by several researchers because of its abundance in cells of nearly all living organism and its association with diabetic complications. Though the effect of glucose on protein glycation has been studied extensively, ribose has received much less attention in protein glycation. Ribose is a naturally occurring sugar, present in all living cells. It has been reported that the amount of ribose present in the body is ~16 mg of ribose per litre of blood (~100 μM)[15] and the concentration of free ribose in human blood plasma is found to be ~7 μM (0-17 μM).[16] Gross ***et al.*** reported the average steady state serum ribose level ranged between 4.8 mg/ 100 ml (83 mg/ kg/h for oral administration) and 81.7 mg/100 ml (222 mg/kg/h for intravenous administration).[17] Ribose is also a major component of many important biomolecules such as riboflavin (i.e., vitamin B2), ribonucleic acid (RNA), and adenosine tri-phosphate (ATP). As ribose is a reducing sugar, it can easily react with proteins to form glycated derivatives. It has been observed that ribose is much more reactive than glucose and other reducing sugars in the formation of AGEs.[18,19] In addition, ribose induces faster glycation over glucose in serum albumin due to its larger fraction of the open-chain form. It has been already reported that glycation in presence of glucose requires a relatively longer time[20] compared to glycation in presence of ribose, which results in the rapid formation of AGEs.

Several compounds are known to inhibit the glycation of proteins. Examples of AGE inhibitors include aminoguanidine[21], aspirin[22], vitamin B_6[23], taurine[24], quercetin[25] and ibuprofen[26] which are able to inhibit AGE formation during the incubation of proteins with glucose ***in vitro***. Identifying compounds having inhibitory activity in the formation of AGEs will help in the prevention of diabetic and other pathogenic complications. However, there are limited reports of the use of nanoparticles as inhibitors of protein glycation. Seneviratne ***et al.*** reported the effect of gold nanoparticles (GNPs) on the non-enzymatic glycation of human serum albumin.[27] Silica-based cerium (III) chloride nanoparticles are also able to prevent the glycation of α-crystallin.[28] In both cases, gold nanoparticles and silica-$CeCl_3$ nanoparticles react with the free amino groups of HSA and ***α***-crystallin respectively and protect them from glycation. The increased use of nanoparticles for therapeutic use has generated interest in the search for compounds that can inhibit glycation in addition to those already mentioned.

Flavonoids are of current interest in research[29,30] because of their multifarious biological and pharmacological properties apart from their antioxidant properties. Fruits, vegetables, and beverages are the main dietary sources of flavonoids.[31,32] Morin is one of the commonly found dietary flavonols. It possesses several biological activities like antioxidant,[33,34] antiproliferative,[35] anticancer,[36] and anti-inflammatory.[37,38,39] Inhibitory activities of naturally occurring flavonoids including morin, in the formation of AGEs have been reported in previous studies.[40,41] However, the poor aqueous solubility of the flavonoids limits its application in biological and pharmaceutical fields.[42] To overcome these issues, morin loaded polylactic-co-glycolic acid nanoparticles (MPNPs) have been prepared[43] to enhance the solubility and bioavailability of morin wherein PLGA acts as a carrier. Based on this background information and considering the role of HSA in our natural immune system, we have monitored the inhibitory effect of morin loaded PLGA NPs on non-enzymatic glycation of HSA in the presence of D-ribose (ribose). The formation of glycated HSA (gHSA) has been monitored for a time period of one month in presence of ribose at physiological temperature and ***pH***. Several spectroscopic techniques such as UV-Vis, fluorescence, circular dichroism and MALDI-ToF measurements have been employed for this study. The inhibitory effect of MPNPs on the formation of advanced glycation end products (AGEs) has also been investigated in addition to its effect on HSA glycation.

Experimental methods

Materials

Human serum albumin (HSA), morin hydrate, polylactic-co-glycolic acid (PLGA), polyvinyl alcohol (PVA) were purchased from Sigma Chemical Co. (St. Louis, USA) and all other analytical grade reagents were obtained from SRL, India. The concentration of HSA was measured spectrophotometrically (UV Shimadzu 1800) by dissolving the protein in 20 mM phosphate buffer of pH 7.0 using a molar extinction coefficient of 35500 M^{-1} cm^{-1} at 280 nm.

Milli-Q grade water was used for all experiments. All experiments have been performed at least three times.

Methods

Preparation of morin loaded PLGA NPs (MPNPs)

We have prepared morin loaded PLGA NPs by a solid in oil in water (S/O/W) emulsification technique[44] with minor modifications. Briefly, 100 mg of PLGA was dissolved in 3 ml ethyl acetate and incubated at room temperature for 2 h. 20 mg of morin was then added to the solution and sonicated for 2 min in a bath sonicator (Oscar Ultrasonic Cleaner, Microclean-101). The organic phase containing morin and PLGA in ethyl acetate was then added dropwise to 6 ml of the aqueous phase containing PVA solution. The stirring was continued for 24 h and finally the prepared NPs were centrifuged and washed with Milli-Q water. The same technique has been used to prepare PLGA nanoparticles.

Characterization of nanoparticles

The NPs were characterized by spectroscopic and microscopic techniques. UV-Vis experiments (UV-1800, Shimadzu) were performed at 25 °C in the range of 200-600 nm. FTIR spectra of NPs were obtained from a Spectrum BX FTIR (Perkin Elmer) equipped with a Lithium Tantalate ($LiTaO_3$) detector and a KBr beam splitter at room temperature. The resolution used was 4 cm^{-1} and the scanning range was from 4000-400 cm^{-1}. The morphology of the NPs was monitored by field emission scanning electron microscopy (FESEM) and atomic force microscopy (AFM). For FESEM, one drop of sample was placed on a glass slide, dried in air and then scanned in a NOVA NANOSEM 450 operating at 10 kV. For AFM measurements, the sample was placed on a freshly cleaved mica foil, air dried and the images taken using Agilent Technologies, Model 5500 in tapping mode using a silicon probe cantilever of 215-235 μm length, at a resonance frequency of 146-236 kHz, and a force constant of 21-98 N/m. To determine the size of the NPs, dynamic light scattering (DLS) studies were performed using a Malvern Nano ZS instrument employing a 4 mW He-Ne laser (λ = 632 nm), with a scattering angle of 173°.

In vitro glycation of HSA

The glycated HSA (gHSA) was prepared ***in vitro*** as described earlier.[45] The human body normally contains 0.53-0.75 mM of serum albumin under physiological conditions.[46] Briefly, gHSA was prepared by incubating 0.6 mM HSA with 50 mM of D-ribose in 100 mM phosphate buffer of pH 7.4 at 37 °C. To prevent bacterial growth during incubation, sodium azide (1 mM) was used as a preservative and added to the above solution. The samples were then incubated in the dark under sterile conditions for a time period of one month. 100 μl aliquots from each sample were withdrawn at 7, 14, 21 and 28 days of incubation and the Amadori adduct level measured.

Detection of glycated products by UV-Vis spectroscopy

UV-Vis absorption spectra of native HSA and gHSA were obtained using a UV-Vis spectrophotometer (UV Shimadzu 1800). The experiment was performed using a quartz cuvette of 1 cm path length at 25 °C at wavelengths ranging from 200 to 600 nm.

Detection of AGE-specific fluorescence

The formation of AGEs of gHSA was monitored by fluorescence spectroscopy. The fluorescence emission spectra of the samples collected at 7, 14, 21 and 28 days of incubation were recorded in a Horiba Jobin Yvon Fluoromax-4 spectrofluorimeter using a 1 cm quartz cell. The formation of AGEs was monitored by measuring the fluorescence of the samples at 430 nm upon excitation at 350 nm. The formation of Argpyrimidine and malonaldialdehyde were monitored by recording the emission spectra of the samples using excitation wavelength values of 320 nm and 370 nm respectively. The excitation and emission slit widths were set at 5 nm and integration time was 0.3 s.

Preparation of reaction incubation mixtures

To test the effects of MPNPs on the glycation of HSA by D-ribose, we have incubated different concentrations of MPNPs with HSA and ribose in 100 mM phosphate buffer of pH 7.4 at 37 °C. These samples were also incubated under similar condition for one month as described earlier and 100 µl aliquots from each sample were taken at 7, 14, 21 and 28 days of incubation to check the Amadori adduct level. When MPNPs were replaced with phosphate buffer, the mixture was termed as a negative control, the replacement of ribose with phosphate buffer provided the sample blank and when both ribose and MPNPs were replaced with phosphate buffer the mixture corresponds to the overall control (blank).

The amount of ribose covalently bound to HSA (phenol–sulfuric acid method)

A phenol-sulfuric acid method has been carried out to monitor the amount of ribose covalently bound to HSA. Briefly, samples were first mixed with concentrated H_2SO_4 and 5% phenol in water. The reaction mixtures were then incubated at 90 °C for 5 min and then cooled to room temperature. The absorbance of the samples was then recorded at 490 nm using UV-Vis spectrophotometer. The inhibitory effect of NPs was then calculated using the following equation:

$$Inhibitory\ rate\ (\%) = 1 - \frac{A_1 - A_3}{A_2 - A_4} \times 100$$

where A_1 is the absorbance of treatment group containing gHSA and MPNPs, A_2 is the absorbance of negative control containing gHSA, A_3 is the absorbance of sample blank containing HSA and MPNPs, A_4 is the absorbance of blank containing HSA only.

Determination of fructosamine (NBT assay)

The nitroblue-tetrazolium (NBT) assay[47,48] was performed to measure the amount of fructosamine, the Amadori product. In brief, gHSA and gHSA treated with MPNPs were incubated with NBT reagent (0.5 mM) in carbonate buffer (100 mM, pH = 10.4) at 37 °C for 15 min. NBT is reduced by fructosamine to obtain a colored reactant, having maximum absorption at 530 nm, which is recorded using a UV-Vis spectrophotometer (UV Shimadzu 1800). The percent inhibition of fructosamine formation by the MPNPs was calculated using the following equation:

$$Inhibitory\ rate\ (\%) = 1 - \frac{A_1 - A_3}{A_2 - A_4} \times 100$$

where A_1 is the absorbance of treatment group containing gHSA and MPNPs, A_2 is the absorbance of negative control containing gHSA, A_3 is the absorbance of sample blank containing HSA and MPNPs, A_4 is the absorbance of blank containing HSA only.

Fluorescence measurement of glycated protein

The aliquots of samples were collected at 7, 14, 21 and 28 days of incubation. The fluorescence emission spectra were recorded in a Horiba Jobin Yvon Fluoromax-4 spectrofluorimeter using a 1 cm quartz cell. The fluorescence intensity of the samples was measured at the excitation wavelength of 350 nm and emission wavelength of 430 nm. The percentage of inhibitory rate was calculated using the following equation

$$Inhibitory\ rate(\%) = 1 - \frac{F_1 - F_3}{F_2 - F_4} \times 100$$

where F_1 is the fluorescence of treatment group containing gHSA and MPNPs, F_2 is the fluorescence of negative control containing gHSA, F_3 is the fluorescence of sample blank containing HSA and MPNPs and F_4 is the fluorescence of blank containing HSA only.

Measurement of free amino group content (OPA assay)

To determine the available amino groups in HSA and gHSA in presence and absence of MPNPs, the *o*-phthalaldehyde (OPA) assay was carried out as described earlier[49] with minor modifications. In brief, the OPA reagent was freshly prepared by mixing 10 ml of 50 mM carbonate buffer pH 10.5, 5 µl of *β*-mercaptoethanol and 5 mg of OPA in 100 µl ethanol and kept in the dark. The samples were then mixed with the OPA reagent and incubated for 2 min at room temperature. The absorbance was then recorded at 340 nm using a UV-Vis spectrophotometer (UV Shimadzu 1800).

Zeta potential measurements

Zeta potential measurements were carried out to monitor the surface charge of MPNPs and HSA bound MPNPs. The analysis was performed using Malvern ZetaSizer Nano ZS instrument at a scattering angle of 173° at 25 °C. The data presented here is the average of three independent readings.

Matrix-assisted laser desorption/ionization time-of-flight (MALDI-ToF) mass spectrometry

The mass of HSA, gHSA and gHSA treated NPs were detected using MALDI-ToF mass spectroscopy. This method has also been used to speculate the possible number of sugar moieties attached to the protein. MALDI-ToF was performed in a Bruker Daltonics Ultraflex

MALDI-ToF/ToF Mass Spectrometer (Germany), using a linear acquisition mode with 3500 shots. The matrix used for MALDI-ToF experiment was prepared by dissolving 20 mg/ml sinapinic acid (3,5-dimethoxy-4-hydroxycinnamic acid) in 50:50 v/v water and HPLC grade acetonitrile containing 0.1% TFA (trifluoroacetic acid) just before the experiment. The samples were then mixed with the matrix solution (1:1 ratio) and a drop of each sample was spotted on the steel plates. The samples were then left to dry for 6 h and the scanning done using an accelerating voltage of 20 kV with an acquisition mass range over an m/z from 30-210 kDa.

Circular dichroism experiments

Far UV-Circular dichroism (CD) experiments were performed to observe changes in secondary structure of HSA, gHSA and gHSA treated with MPNPs. CD analyses were carried out in a Jasco J-815 spectrometer using a 1 cm path length quartz cuvette. The spectra were obtained in the far UV region between 190 to 240 nm at a scan rate of 50 nm/min and a response time of 4 s keeping the concentration of protein fixed at 2 µM. DICHROWEB, an online server[50] has been used to estimate the protein secondary structure content. A 20 mM phosphate buffer (pH 7.4) solution was used as the blank to normalize the baseline of each reading.

Results and discussion

Preparation and characterization of nanoparticles

To study the antiglycation effect of nanoparticles on protein glycation, we have prepared morin loaded PLGA NPs (MPNPs) and characterized them via UV-Vis spectroscopy, FTIR, FESEM, AFM and DLS (Figure 1). From the UV-Vis spectroscopy study, the two major absorption peaks of morin were found at 351 nm (due to the cinnamoyl moiety) and 264 nm (due to the benzoyl moiety) but the peak at 351 nm of morin shifted to 393 nm after the formation of NPs. The presence of both the peaks of morin in the prepared NPs

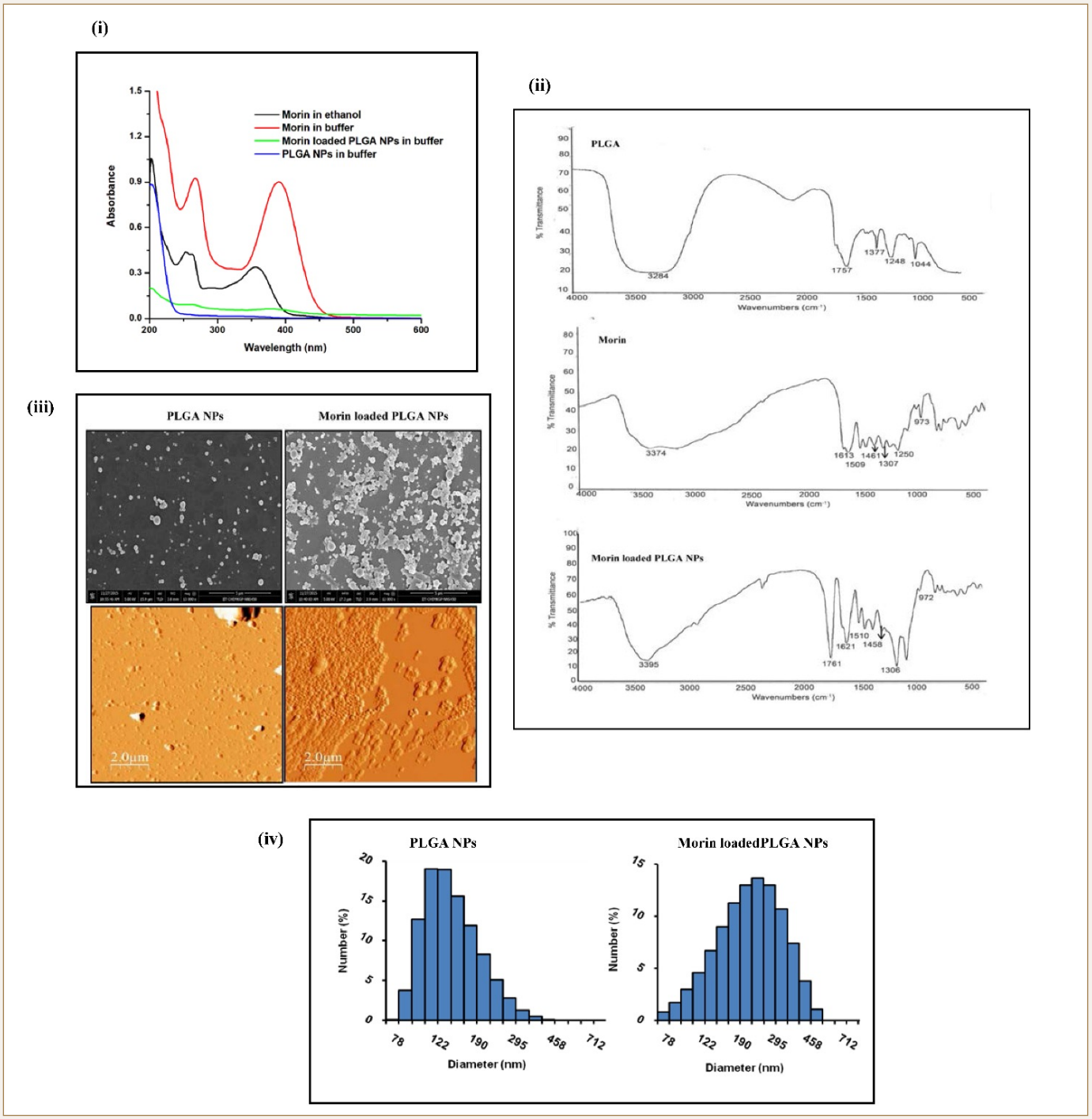

Figure 1. Characterization of morin loaded PLGA NPs (i) UV-Vis absorption spectra (ii) FTIR spectra (iii) FESEM and AFM images (iv) DLS measurements.

confirms the unaltered chemical structure of morin after encapsulation. The FTIR spectrum of PLGA exhibits several characteristic peaks around 1757 cm^{-1} (due to the C=O stretching frequency), 1044 cm^{-1} and 1248 cm^{-1} (due to the C–O stretching frequency). Morin shows a strong intensity band at 3374 cm^{-1} (due to the –OH group). The bands at 1613 cm^{-1}, 1509 cm^{-1} and 1461 cm^{-1} are assigned to the C=C stretching vibration in the aromatic ring. The –COH deformation vibration is observed at 1307 cm^{-1} and bands at 1250 cm^{-1} and 973 cm^{-1} involve the –C-OH stretching vibration. The spectra of morin loaded PLGA NPs shows the characteristic peaks of morin with almost negligible shifts at 1621, 1510, 1458, 1306 and 972 cm^{-1} and the specific functional groups of PLGA in the prepared NPs have almost the same characteristic peaks of pure PLGA. Thus, from FTIR analysis, it appears that morin is entrapped within the PLGA matrix without altering its chemical structure. This result is also in agreement with the finding that has been shown from our laboratory, where fisetin loaded human serum albumin (HSA) nanoparticles showed similar results.

The morphology of the NPs was then visualized by field emission scanning electron microscopy (FESEM) and atomic force microscopy (AFM) which are shown in Figure 1 (iii). FESEM images revealed that NPs were homogeneous, smooth and spherical in morphology. AFM images also confirmed the smooth topography of the NPs. The sizes of the NPs were determined by dynamic light scattering (DLS) from which it was found the average size of PLGA NPs is 131±9 nm and that of morin loaded PLGA NPs is 237±17 nm.

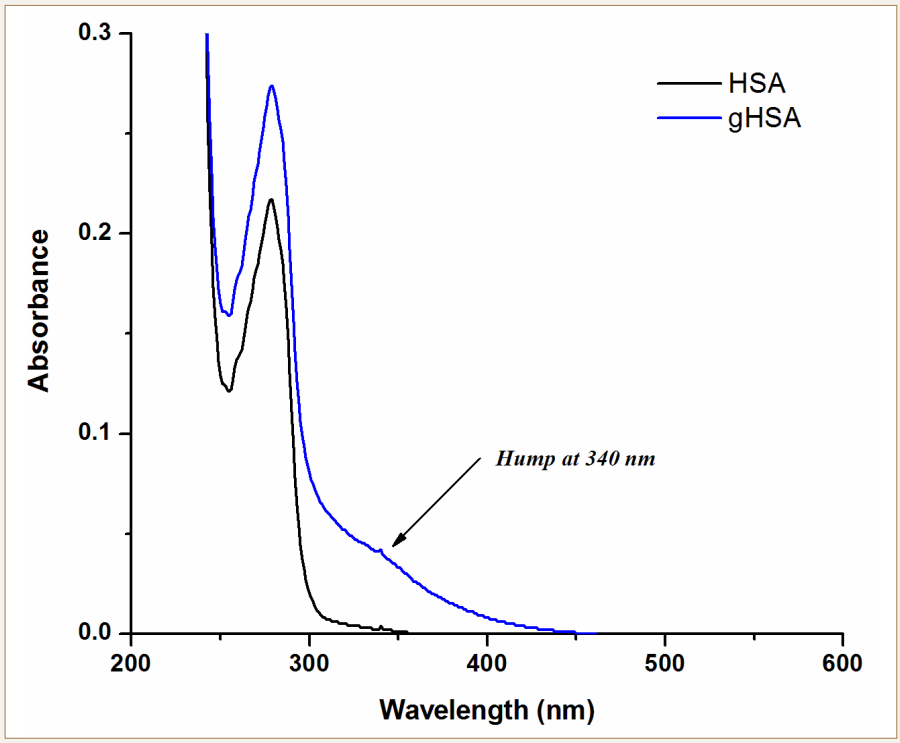

Figure 2. UV-Vis absorption spectra of HSA and glycated HSA; Hump at 340 nm indicating the formation of AGEs.

Characterization of glycated HSA

HSA was incubated with and without D-ribose for 28 days at 37 °C. After 28 days of incubation, a distinct brown color observed for ribose modified samples which indicates that there is an involvement of the Maillard reaction. HSA showed a characteristic peak at 280 nm whereas gHSA showed an increase in absorbance at 280 nm and a hyperchromicity of 27% was observed. HSA, incubated without sugar does not show any absorbance in between 300-400 nm whereas HSA incubated with ribose shows absorbance near 340 nm. The appearance of a small hump at 340 nm (Figure 2) in gHSA also indicates the formation of AGEs. Previous reports have also shown that the formation of AGEs results in an increase in absorbance in the range (300-400) nm.[52,53]

To monitor the presence of different kinds of advanced glycation end products (AGEs) fluorescence spectroscopic techniques have been employed. The different AGEs such as Argpyrimidine, and malonaldialdehyde were distinguished by recording their emission intensities at 410 nm (λ_{ex} 320 nm) and 450 nm (λ_{ex} 370 nm) respectively (Figure 3). The fluorescence emission intensities of

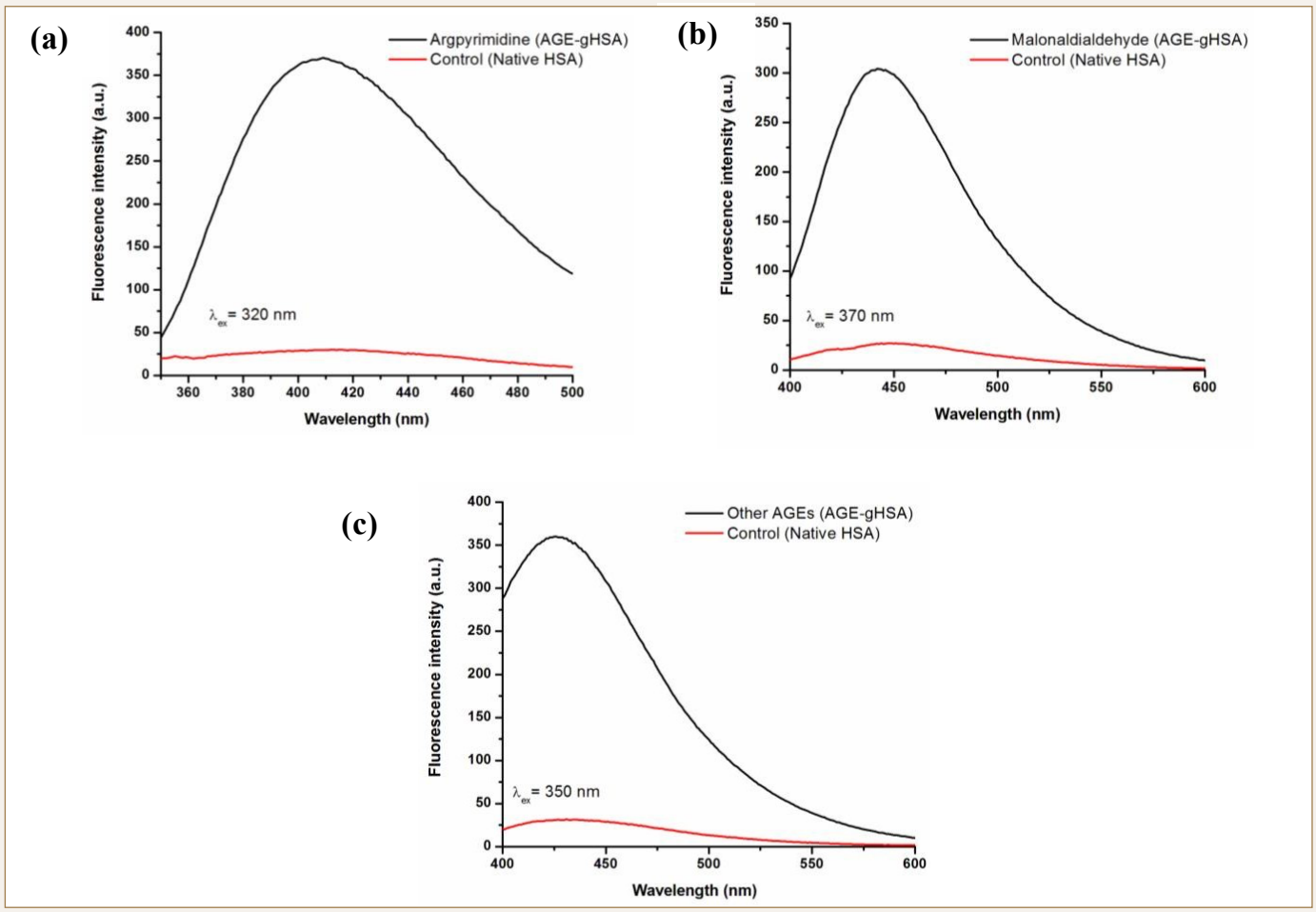

Figure 3. Fluorescence emission spectra of formation of (a) argpyrimidine, (b) malonaldialdehyde and (c) other AGEs after the glycation over 30 days. λex = 320, 370 and 350 nm for (a), (b) and (c) respectively.

other different AGE products were monitored by taking their emission intensities at 430 nm upon excitation at 350 nm (Figure 3). These observations confirm the formation of AGEs by the reaction of protein with ribose.

Figure 4 (a) shows the trends in fluorescence intensities of HSA incubated with ribose at different time intervals. An increase in fluorescence intensity with increasing time of incubation indicates that the formation of AGEs increases with increase in incubation time. We have also found a noticeable decrease in the Trp fluorescence intensity (~ 62%) in gHSA (Figure 4b) which is similar to the result that has been described earlier.[54]

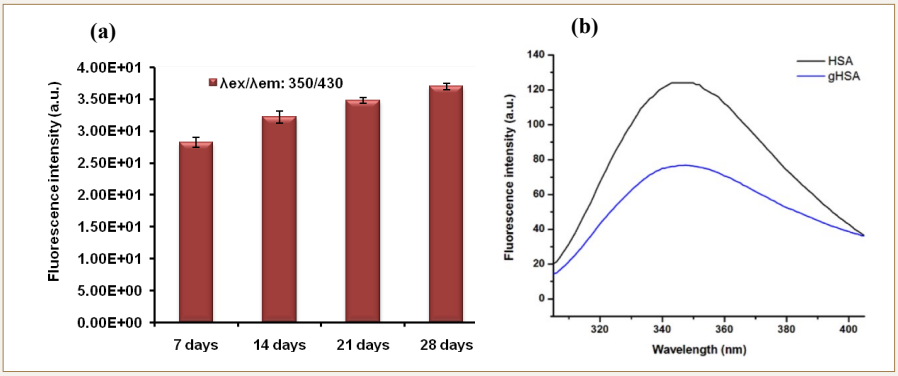

Figure 4. (a) Fluorescence intensities of HSA incubated with 30 mM of D-ribose at different time intervals **(b)** Fluorescence emission spectra of HSA and glycated HSA: λex = 295 nm.

Inhibitory effect of NPs on protein glycation

The main objective of the present investigation was to explore the use of NPs as suitable AGEs inhibitor by providing proper evidences. Figure 5 shows the schematic representation of the inhibitory effect of MPNPs on protein glycation. Protein glycation generally passes through early, intermediate and advanced stages. In this regard, the inhibitory effect of NPs in different stages was distinguished by calculating the amount of ribose covalently bound onto HSA, formation of fructosamine and other fluorescent products after incubation at different concentrations of NPs with HSA and ribose at 37 °C for 28 days.

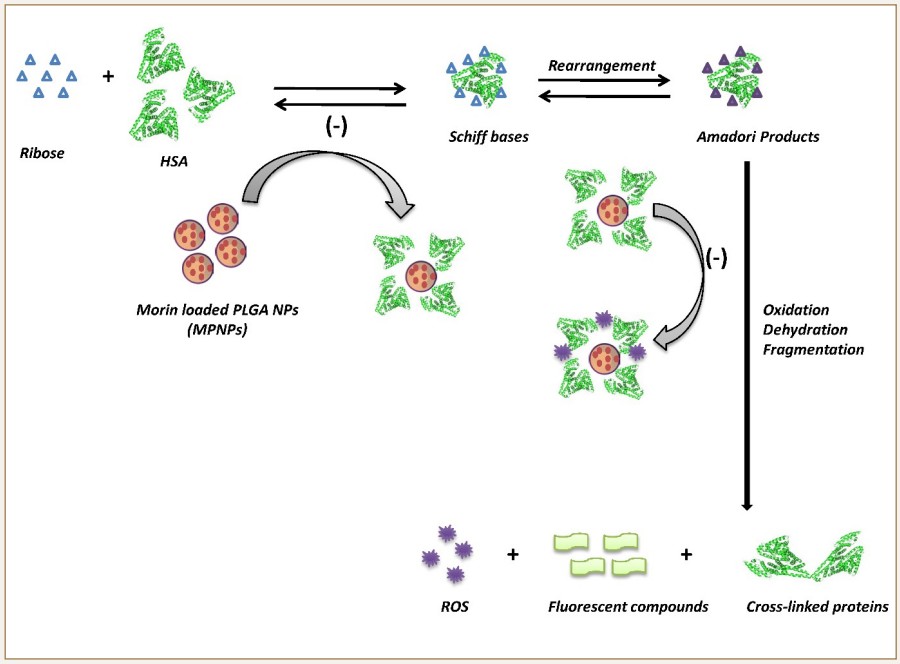

Figure 5. Schematic representation of the inhibitory effect of MPNPs on protein glycation.

UV-Vis spectroscopy

HSA, incubated without sugar showed a characteristic peak at 280 nm whereas gHSA showed an increase in absorbance at 280 nm. Figure 6 shows the UV-Vis spectra of HSA and gHSA in presence and absence of different concentrations of MPNPs incubated for 28 days in 100 mM phosphate buffer pH 7.4 at 37 °C. As shown in Figure 6, we have observed that gHSA incubated with the different concentrations of MPNPs has lower absorbance than that of gHSA which suggests that MPNPs are able to inhibit glycation.

Phenol-sulfuric acid assay

Initially the carbonyl group of ribose is covalently bound with the free amino groups of HSA. The extent of protein glycation is thus affected by the amount of ribose covalently bound to HSA. The phenol-sulfuric acid assay was performed to determine the amount of ribose covalently bound to HSA. According to this method, carbohydrates like simple sugars, oligosaccharides, polysaccharides, and their derivatives react in presence of concentrated sulfuric acid and heat to produce furan derivatives. In presence of phenol, the furan derivatives produce stable yellow gold colored compounds (Figure 7)

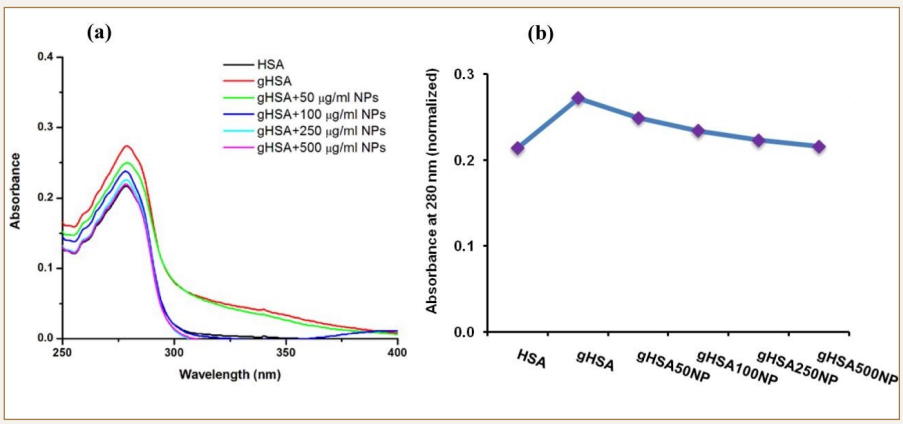

Figure 6. (a) UV-Vis absorption spectra of HSA and gHSA in presence and absence of different concentrations of MPNPs incubated for 28 days in 100 mM phosphate buffer pH 7.4 at 37 °C and **(b)** corresponding normalized plot at 280 nm absorbance.

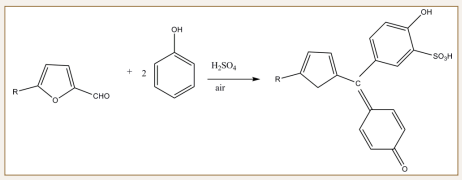

Figure 7. Mechanism of Phenol-sulphuric acid assay.

which show maximum absorbance at 490 nm. From this assay, we have observed that, there is an increment in the absorbance of HSA at 490 nm after incubation with ribose, indicating that HSA interacts with ribose and protein glycation occurs. However, MPNPs decrease the absorbance at 490 nm. The inhibitory rate of ribose covalently bound to HSA in presence of MPNPs is given in Figure 8. The results show that the percentage of inhibition increases with increase in concentration of MPNPs. MPNPs at a concentration of 50 µg/ml shows 73±1.5% inhibition whereas 500 µg/ml of MPNPs shows 87±0.9% inhibition. Thus, inhibition occurs in a dose dependent manner and NPs are able to inhibit protein glycation at the early stage. increases with increase in concentration of MPNPs in both cases. The inhibitory rate of fructosamine formation and fluorescent products formation is 43±2.4% and 54±2.0% respectively at 500 µg/ml conc. of MPNPs. Figure 10 shows the histogram of fluorescence intensities of AGEs formation of HSA and gHSA in absence and presence of different concentrations of MPNPs at different time intervals. We have observed that AGEs formation increases with increase in incubation time. The results also suggest that inhibition occurs in a dose dependent manner.

Thus, by calculating (i) the amount of ribose bound to HSA (in the early stage); (ii) fructosamine formation (in the intermediate stage) and (iii) fluorescent product formation (in the advanced stage), we have observed the inhibitory role of NPs on protein glycation at different stages. To analyze the effect of MPNPs in the various stages of protein glycation, we have also determined the increase in inhibitory rate at each stage. The increase in inhibitory rate at each stage is denoted as δE, δI, δA where δE represents the inhibitory rate of ribose, δI represents the (inhibitory rate of fructosamine - that of ribose) and δA represents the (inhibitory rate of fructosamine - that of fluorescent products). The calculated δE, δI, δA values are shown in Table 1 and we observed that δE > δA > δI at all concentrations.

This implies that MPNPs inhibit protein glycation mostly at the early stage, then at the advanced stage but there is no effect at the intermediate stage which means that MPNPs are unable to stop the rearrangement of Schiff bases into Amadori products. Our observation is also in agreement with the previous results[55,56,57] where it has been shown that aminoguanidine, Se NPs and the ethyl acetate extract of *Teucrium polium* act as antiglycating agents but fail to inhibit the formation of Amadori products.

Free amino group detection

We have determined the available amino groups in HSA and gHSA in presence and absence of MPNPs by o-phthalaldehyde (OPA) assay. As shown in Figure 11, we have observed that there is a reduction

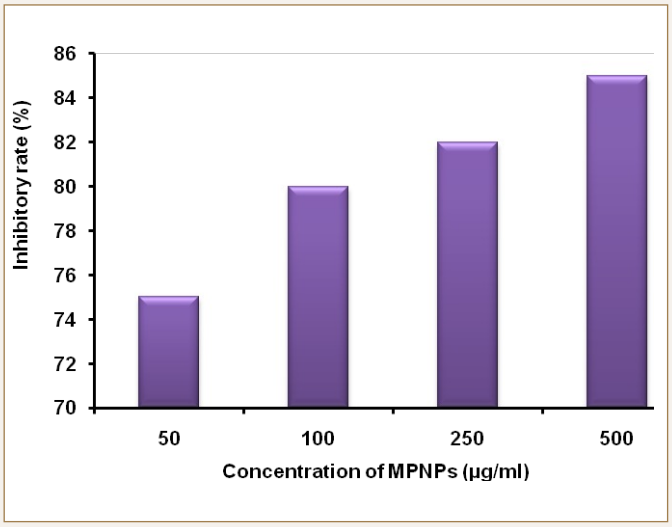

Figure 8. The inhibitory rate of ribose covalently bound to HSA in presence of MPNPs.

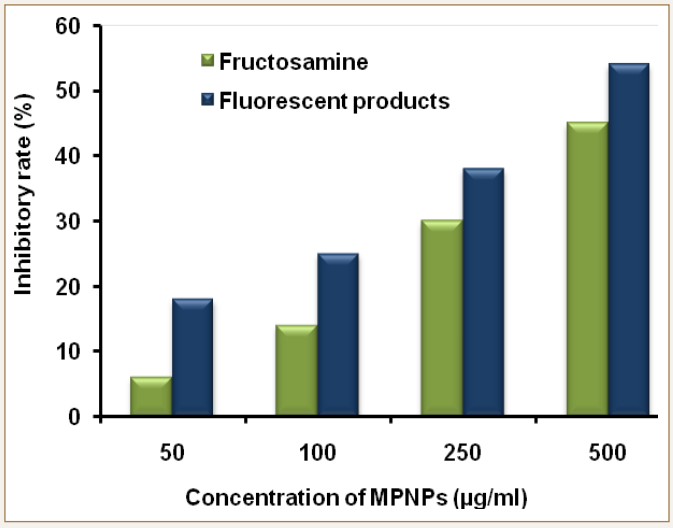

Figure 9. Inhibitory effect of MPNPs on the formation of fructosamine and fluorescent products.

Determination of fructosamine and fluorescent products

The formation of fructosamine was determined by a nitroblue-tetrazolium (NBT) assay. This is a colorimetric test-based assay where NBT in an alkaline solution is reduced by fructosamine to form a colored monoformazan dye which gives an absorption maximum at 530 nm. Fluorescence spectroscopy was used to observe the formation of AGEs that are fluorescent products. We have calculated the inhibitory rate of MPNPs on the formation of fructosamine and the fluorescent products using the formulae stated above. As shown in Figure 9, we have observed that the percentage of inhibition

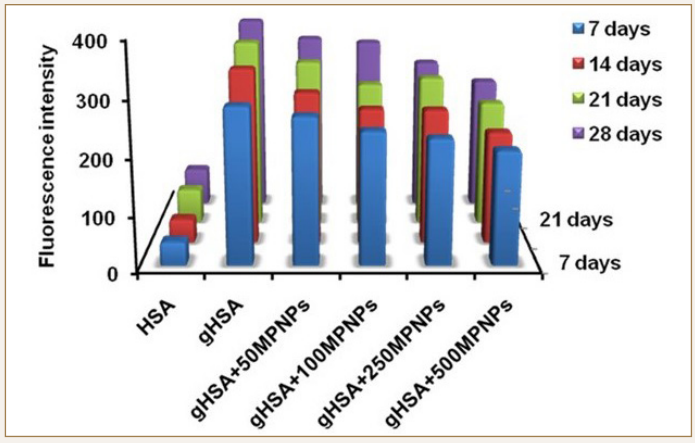

Figure 10. Fluorescence intensities of HSA and gHSA in absence and presence of different concentrations of MPNPs at different time intervals.

Table 1. Increase of inhibitory rate in each stage of glycation

Concentration of MPNPs (μg/ml)	δE (%)	δI (%)	δA (%)
50	73±1.5	-65±2.3	9±3.3
100	78±1.1	-61±2.6	11±1.7
250	83±1.2	-52±1.7	13±2.6
500	87±0.9	-43±2.7	10±0.8

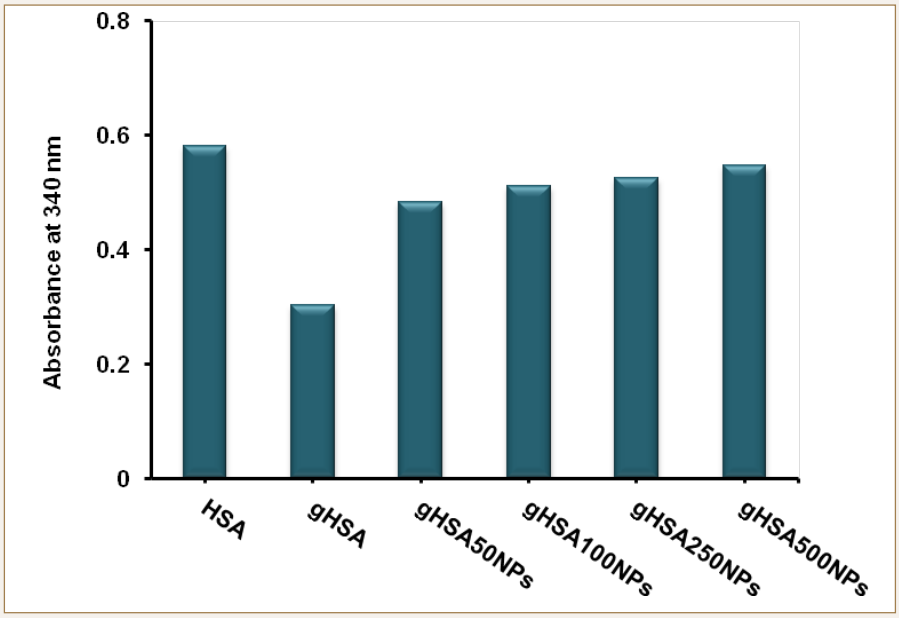

Figure 11. Protective effect of MPNPs on the available amino groups in HSA.

in the absorbance at 340 nm in case of gHSA than HSA. However, the presence of MPNPs results in an increase in absorbance at 340 nm. The measurement of free amino groups (Figure 11) indicates that there were approximately 50% less free amino groups in gHSA than in HSA. However, the presence of MPNPs helps in protecting the free amino groups of HSA from reacting with ribose, thereby preventing AGE formation.

Proposed mechanism for the inhibitory effect of MPNPs in the early and intermediate stage

When the nanoparticles enter into body, they come in contact with the protein present in plasma and the protein immediately binds on the surface of the nanoparticles. Human serum albumin (HSA) is one of the most abundant plasma proteins. At experimental pH (pH 7.4), HSA (pI ~4.9) is negatively charged. Instantaneous protein adsorption generally causes a small increment in the particle size. Further the zeta potential of NPs is also shifted towards the positive value after the adsorption of protein onto the nanoparticles. MPNPs and HSA-MPNPs complex showed negative surface charge of around –27±2 mV and –20±1 mV respectively. A noticeable increase in the zeta potential of HSA-MPNPs complex and a slight increase in the size of HSA-MPNPs complex indicate that HSA is adsorbed on the surface of MPNPs. In the early stage, a Schiff base is formed between the free amino group of HSA and the carbonyl group of ribose. However, in presence of MPNPs, HSA is adsorbed on the surface of NPs before formation of the Schiff base with ribose which simultaneously inhibits protein glycation. This is further confirmed through an FTIR technique.

Figure 12 shows the FTIR spectra of collected MPNPs after centrifugation, MPNPs and HSA. For HSA, the peaks at 1654 cm^{-1}, 1540 cm^{-1} and 1385 cm^{-1} are assigned to the Amide I band (due to the C=O stretching frequency), Amide II band (due to C-N stretching coupled with N-H bending) and Amide III band (due to C-N stretching vibrations) respectively. The spectra of morin loaded PLGA NPs show characteristic peaks at 1621 cm^{-1}, 1510 cm^{-1}, 1458 cm^{-1}, 1306 cm^{-1} and 972 cm^{-1} whereas in the spectrum of the collected NPs after centrifugation a new peak around 1655 cm^{-1} and 1438 cm^{-1} appear which is the indication of the interaction of C=O and C-N groups of HSA and MPNPs. In addition, the peaks of –NH at 3081 cm^{-1} and 1540 cm^{-1} in HSA disappear in the spectrum of collected MPNPs which indicates the interaction between surface of MPNPs and –NH groups in HSA. From these results, we can

conclude that MPNPs can bind to the free amino groups of HSA and most likely protect them from glycation in the early stages as mentioned earlier.

A number of studies have reported that in the presence of the oxygen superoxide radical, anions are formed from Amadori products by glycoxidation.[58,59,60,-61] From previous reports, it is clear that ROS are not only formed during the advanced stage of glycation but is also the cause for which further glycation occurs. It has also been reported that compounds having antioxidants and radical scavenging properties are able to inhibit protein glycation.[62,63,64,65] We have shown that MPNPs have free radical scavenging activity against DPPH free radicals, which help us to conclude that the inhibition of formation of AGEs during the advanced stage of glycation may be because of the radical scavenging property of MPNPs.

Determination of the number of attached ribose moieties: MALDI-ToF studies

MALDI-ToF spectroscopy experiment was carried out to determine the number of ribose moieties attached to HSA (Figure 13). The number of sugar moieties attached during glycation can be calculated based on the following equation: number of sugar adducts = (molar mass of glycated protein - molar mass of native protein)/molar mass of sugar. The MALDI-ToF spectra of native HSA showed a wide band centered at an m/z of 66507 Da and that of glycated HSA exhibited a narrow band centered at an m/z of 67631 Da. There is an increase in mass shift of 1124 Da in case of gHSA which means that 7 ribose moieties are attached to HSA during the process of glycation. However, a significant decrease in the mass shift of HSA occurs when MPNPs were added to gHSA. The results showed that there is a noticeable decrease in the number of ribose adducts from 7 sugar molecules (control solution) to 2 (500 μg/ml MPNPs) which suggests that MPNPs has inhibitory effect on nonenzymatic glycation of protein.

Secondary Structure Analysis by CD

The changes in the secondary structure of HSA, gHSA and the glycated protein samples in presence of different concentrations of MPNPs was evaluated using circular dichroism spectroscopy in the range

of 190–240 nm. The spectrum showed two negative bands, one at 208 nm and another at 222 nm, which are the characteristic features of α-helical content of the protein. The incubation of HSA with ribose for 28 days results in a decrease in the α-helical content of native HSA from 58±1.3% to 50.2±0.7% as calculated via online server DICHROWEB using SELCON analysis program. However, the incubation of HSA and ribose with different concentrations of MPNPs further increases the α-helical content. A comparison of the CD results suggests that HSA had the maximum α-helical content, while gHSA showed a loss in α-helical content upon modification by ribose. Further MPNPs treatment protect HSA from alterations in the secondary structure and the extent of α-helix content exhibited less change when incubated with 500 µg/ml MPNPs.

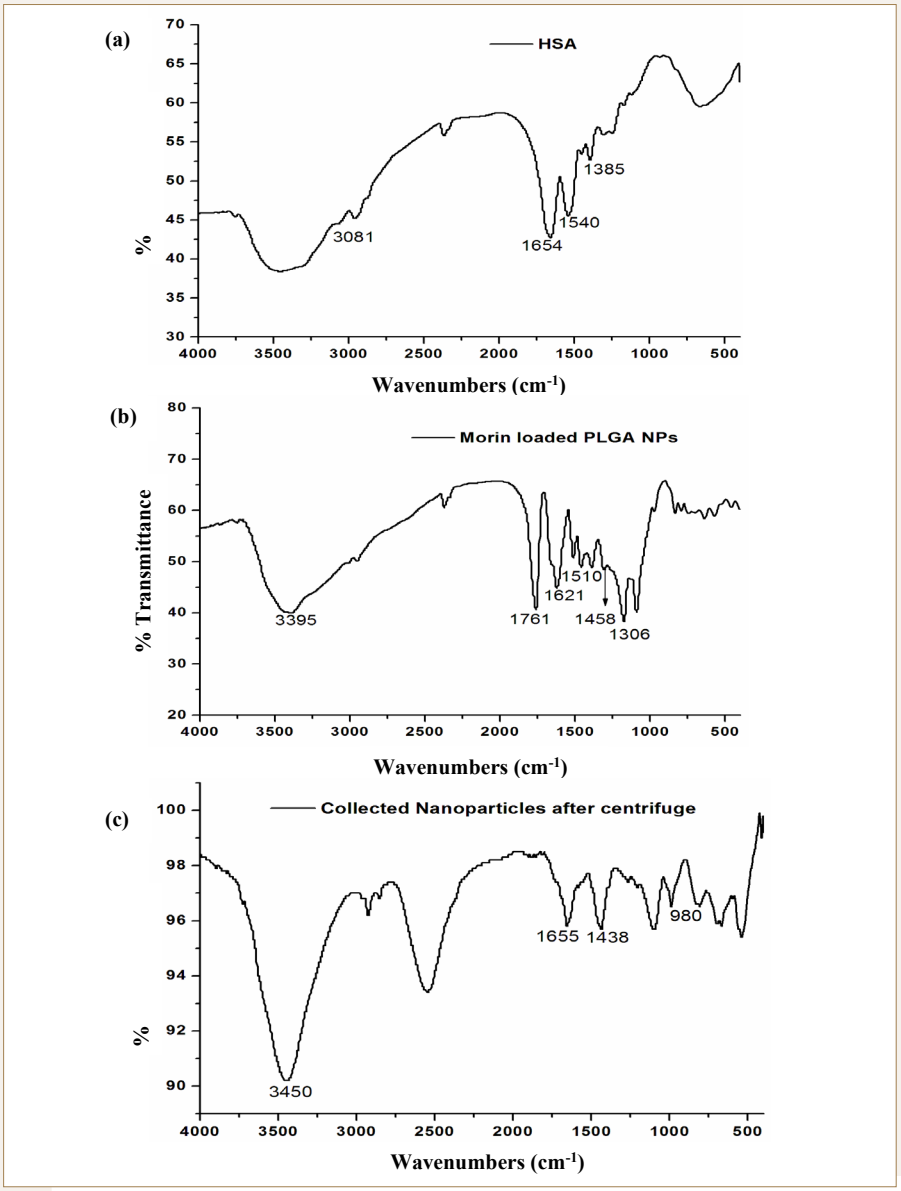

Figure 12. FTIR spectra of **(a)** HSA **(b)** Morin loaded PLGA NPs and **(c)** collected MPNPs. Collected MPNPs are obtained through centrifugation, washing and drying the NPs that are incubated with HSA and ribose for 28 days at 37 °C.

Table 2. Estimation of α-helical content (%) via online server DICHROWEB using SELCON analysis program

Systems	% α-helix
HSA	58±1.3
gHSA	50.2±0.7
gHSA+50 µg/ml MPNPs	51.1±0.3
gHSA+100 µg/ml MPNPs	51.7±0.22
gHSA+250 µg/ml MPNPs	54.5±0.19
gHSA+500 µg/ml MPNPs	57.3±0.42

The CD spectra of HSA and gHSA in the presence or absence of different concentrations of MPNPs are shown in Figure 14. Table 2 shows the percentage of *α*-helical content of HSA and gHSA in absence and presence of different concentrations of MPNPs.

Conclusion

In summary, we have investigated for the first time the inhibitory effect of morin loaded PLGA NPs (MPNPs) on the D-ribose induced protein glycation. Our results showed that MPNPs protect the free amino groups of the model protein HSA from reacting with ribose, thereby preventing AGE formation and MPNPs also decreases the level of fructosamine. During incubation of HSA and ribose in presence of MPNPs, HSA is adsorbed on the surface of NPs before formation of a Schiff base with ribose which simultaneously inhibits protein glycation. This has been further confirmed through FTIR studies. We have compared the increase in the inhibitory rate in various stages and the greatest inhibitory effect of MPNPs was found in the early stage followed by the advanced stage whereas there is no effect in the intermediate stage of the glycation procedure. The incubation of HSA and ribose with different concentrations of MPNPs helps in increasing the α-helical content, thereby protecting HSA from any deviation in its secondary structure. Most of the research in this field is carried out through *in vitro* experimental studies and further investigations are warranted to explore the *in vivo* efficacy of these antiglycating compounds in suitable animal model. We believe that our observations will be beneficial for potential studies in the investigations of the *in vivo* role of MPNPs.

Acknowledgements

SD is grateful to Science and Engineering Research Board (SERB) for partial funding. The authors would like to acknowledge the Central Research Facility, IIT Kharagpur for providing experimental facilities. PG thanks CSIR, New Delhi for her fellowship.

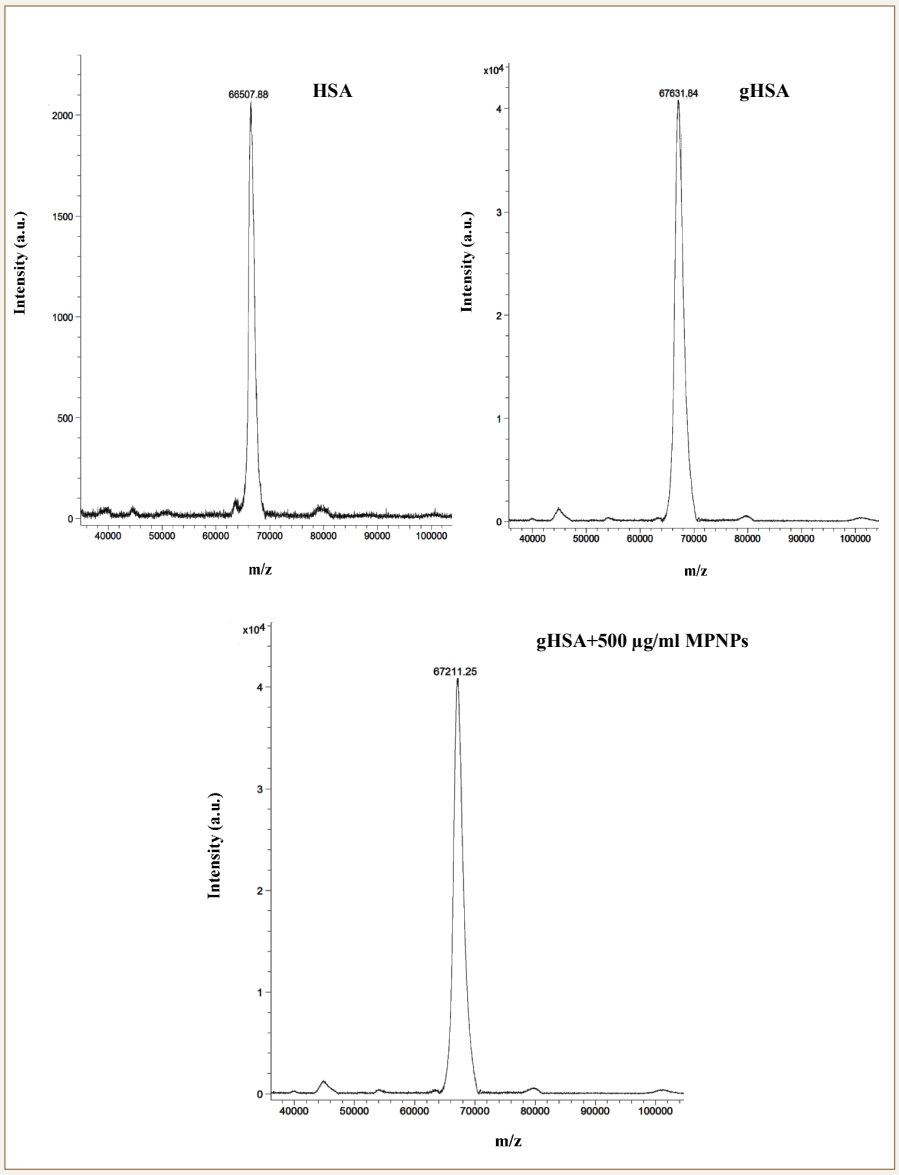

Figure 13. MALDI-ToF mass spectra of (a) native HSA (b) HSA incubated with D-ribose and (c) HSA incubated with D-ribose in presence of 500 µg/ml of MPNPs.

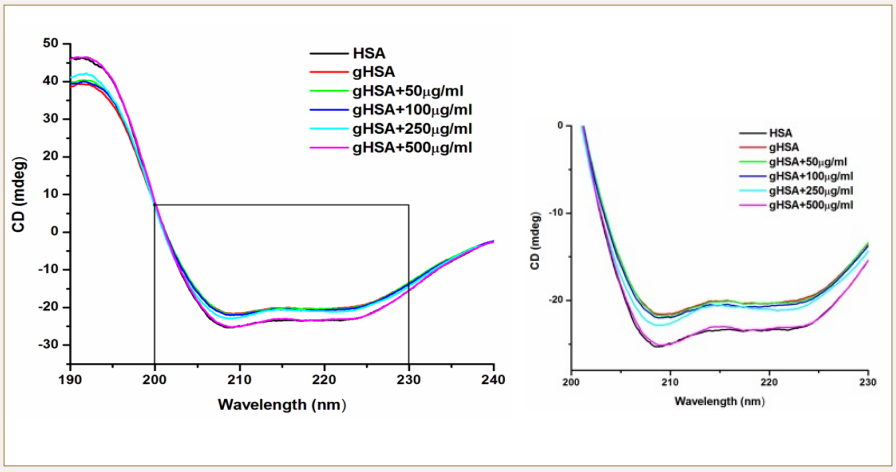

Figure 14. CD spectra of HSA and gHSA in the presence or absence of different concentrations of MPNPs.

to Healthy Persons and to Patients with Myoadenylate Deaminase Deficiency. *Klin Wochenschr* **1989**, *67*, 1205-1213.
18. Syrovy, I. Glycation of albumin: reaction with glucose, fructose, galactose, ribose or glyceraldehyde measured using four methods. *J Biochem. Biophys. Methods* **1994**, *28*, 115- 121.
19. Khalifah, R. G.; Todd, P.; Booth, A. A.; Yang, S. X.; Mott, J. D.; Hudson, B. G. Kinetics of nonenzymatic glycation of ribonuclease A leading to advanced glycation end products, Paradoxical inhibition by ribose leads to facile isolation of protein intermediate for rapid post-Amadori studies. *Biochemistry* **1996**, *35*, 4645-4654.
20. Monnier, V. M.; Cerami, A. Nonenzymatic browning in vivo: possible process for aging of long-lived proteins. *Science* **1981**, *211*, 491-493.
21. Brownlee, M.; Vlassara, H.; Kooney, A.; Ulrich, P.; Cerami, A. Aminoguanidine prevents diabetes-induced arterial wall protein cross-linking. *Science* **1986,** *232*, 1629-1632.
22. Huby, R.; Harding, J. J. Non-enzymic glycosylation (glycation) of lens proteins by galactose and protection by aspirin and reduced glutathione. *Exp. Eye. Res.* **1988,** *47*, 53-59.
23. Booth, A. A.; Khalifah, R. G.; Hudson, B. G. Thiamine pyrophosphate and pyridoxamine inhibit the formation of antigenic advanced glycation end-products: comparison with aminoguanidine. *Biochem. Biophys. Res. Commun.* **1996**, *220*, 113-119.
24. Malone, J. I.; Lowitt, S.; Cook, W. R. Nonosmotic diabetic cataracts. *Pedatr. Res.* **1990**, *27*, 293-296
25. Morimitsu, Y.; Yoshida, K.; Esaki, S.; Hirota, A. Protein glycation inhibitors from thyme (Thymus vulgaris). *Biosci. Biotechnol. Biochem.* **1995**, *59*, 2018-2021.
26. Raza, K.; Harding, J. J. Non-enzymic modification of lens proteins by glucose and fructose: effects of ibuprofen. *Exp. Eye Res.* **1991**, *52*, 205-212.
27. Seneviratne, C.; Narayanan, R.; Liu, W.; Dain, J. A. The *in vitro* inhibition effect of 2 nm gold nanoparticles on non-enzymatic glycation of human serum albumin. *Biochem. Biophys. Res. Commun.* **2012**, *422*, 447-454
28. Yang, J.; Cai, L.; Zhang, S.; Zhu, X.; Zhou, P.; Lu, Y. Silica-based cerium (III) chloride nanoparticles prevent the fructose-induced glycation of a-crystallin and H_2O_2-induced oxidative stress in human lens epithelial cells. *Arch. Pharm. Res.* **2014**, *37*, 404-411.
29. Ghosh, P.; Bag, S.; Roy, A. S.; Subramani, E.; Chaudhury, K.; Dasgupta, S. Solubility enhancement of morin and epicatechin through encapsulation in an albumin based nanoparticulate system and their anticancer activity against the MDA-MB-468 breast cancer cell line. *RSC Adv.* **2016**, *6*, 101415-101429.
30. Ghosh, P.; Bag, S.; Parveen, S.; Subramani, E.; Chaudhury, K.; Dasgupta, S. Nanoencapsulation as a Promising Platform for the Delivery of the Morin-Cu (II) Complex: Antibacterial and Anticancer Potential. *ACS Omega* **2022**, *7*, 7931-7944.
31. Lampe, J. W. Spicing up a vegetarian diet: chemopreventive effects of phytochemicals. *Am. J. Clin. Nutr.* **2003**, *78*, 579S-583S.
32. Prior, R. L. Fruits and vegetables in the prevention of cellular oxidative damage. *Am. J. Clin. Nutr.* **2003**, *78*, 570S-578S.
33. Prahalathan, P.; Kumar, S.; Raja, B. Morin attenuates blood pressure and oxidative stress in deoxycorticosterone acetate-salt hypertensive rats: a biochemical and histopathological evaluation. *Metabolism* **2012**, *61*, 1087-1099.
34. Merwid-Lad, A.; Trocha, M.; Chlebda, E.; Sozanski, T.; Magdalan, J.; Ksiadzyna, D.; Kopacz, M.; Kuzniar, A.; Nowak, D.; Piesniewska, M. Effects of morin-5'-sulfonic acid sodium salt (NaMSA) on cyclophosphamide-induced changes in oxidoredox state in rat liver and kidney. *Hum Exp Toxicol* **2012**, *31*, 812-819.
35. Kuo, H. M.; Chang, L. S.; Lin, Y. L.; Lu, H. F.; Yang, J. S.; Lee, J. H.; Chung, J. G. Morin inhibits the growth of human leukemia HL-60 cells via cell cycle arrest and induction of apoptosis through mitochondria dependent pathway, *Anticancer Res* **2007**, *27*, 395-406.
36. Brown, J.; O'Prey, J.; Harrison, P. R. Enhanced sensitivity of human oral tumours to the flavonol, morin, during cancer progression: involvement of the Akt and stress kinase pathways. *Carcinogenesis* **2003**, *24*, 171-177.
37. Francis, A. R.; Shetty, T. K.; Bhattacharya, R. K. Modulating effect of plant flavonoids on the mutagenicity of *N*-methyl-*N*-nitro-N-nitrosoguanidine. *Carcinogenesis* **1989**, *10*, 1953-1955.
38. Hanasaki, Y.; Ogawa, S.; Fukui, S. The correlation between active oxygens scavenging and antioxidative effects of flavonoids. *Free Radic. Biol. Med.* **1994**, *16*, 845-850.
39. Fang, S. H.; Hou, Y. C.; Chang, W. C.; Hsiu, S. L.; Chao, P. D.; Chiang, B. L. Morin sulfates/glucuronides exert anti-inflammatory activity on activated macrophages and decreased the incidence of septic shock. *Life Sci.* **2003**, *74*, 743-756.
40. Sasaki, K.; Chiba, S.; Yoshizaki, F. Effect of natural flavonoids, stilbenes and caffeic acid oligomers on protein glycation. *Biomed Rep.* **2014**, *2*, 628-632.
41. Zeng, L.; Zhang, G.; Liao, Y.; Gong, D. Inhibitory mechanism of morin on α-glucosidase and its anti-glycation properties. *Food Funct.* **2016**, *7*, 3953-3963.
42. Ghosh, P.; Bag, S.; Roy, P.; Chakraborty, I.; Dasgupta, S. Permeation of flavonoid loaded human serum albumin nanoparticles across model membrane bilayers. *Int. J. Biol. Macromol.* **2022**, In Press. DOI: https://doi.org/10.1016/j.ijbiomac.2022.09.186.
43. Ghosh, P.; Patwari, J.; Dasgupta, S. Complexation With Human Serum Albumin Facilitates Sustained Release of Morin From Polylactic-Co-Glycolic Acid Nanoparticles. *J. Phys. Chem. B* **2017**, *121*, 1758-1770.
44. Xie, X.; Tao, Q.; Zou, Y.; Zhang, F.; Guo, M.; Wang, Y.; Wang, H.; Zhou, Q.; Yu, S. PLGA nanoparticles improve the oral bioavailability of curcumin in rats: characterizations and mechanisms. *J Agric Food Chem.* **2011**, *59*, 9280-9289.
45. Joseph, K. S.; Anguizola, J.; Hage, D. S. Binding of tolbutamide to glycated human serum albumin. *J. Pharm. Biomed. Anal.* **2011**, 54, 426-432.
46. Fasano, M.; Curry, S.; Terreno, E.; Galliano, M.; Fanali, G.; Narciso, P.; Notari, S.; Ascenzi, P. The extraordinary ligand binding properties of human serum albumin. *IUBMB Life.* **2005**, *57*, 787-796.
47. Baker, J. R.; Zyzak, D. V.; Thorpe, S. R.; Baynes, J. W. Chemistry of the fructosamine assay: D-glucosone is the product of oxidation of Amadori compounds. *Clin. Chem.* **1994**, *40*, 1950-1955.
48. Johnson, R. N.; Metcalf, P. A.; Baker, J. R. Fructosamine: A new approach to the estimation of serum glycosylprotein. An index of diabetic control. *Clin. Chim. Acta* **1983**, *127*, 87-95.
49. Fayle, S. E.; Healy, J. P.; Brown, P. A.; Reid, E. A.; Gerrard, J. A.; Ames, J. M. Novel approaches to the analysis of the Maillard reaction of proteins. *Electrophoresis* **2001**, *22*, 1518-1525.
50. Whitmore, L.; Wallace, B. A. DICHROWEB, an online server for protein secondary structure analyses from circular dichroism spectroscopic data. *Nucleic Acids Res.* **2004**, *32*, W668-73.
51. Ghosh, P.; Roy, A.S.; Chaudhury, S.; Jana, S.K.; Chaudhury, K.; Dasgupta, S. Preparation of albumin-based nanoparticles for delivery of fisetin and evaluation of its cytotoxic activity. *Int J Biol Macromol.* **2016**, *86*, 408-417.
52. Ashraf, J. M.; Ansari, M. A.; Khan, H. M.; Alzohairy, M. A.; Choi, I. Green synthesis of silver nanoparticles and characterization of their inhibitory effects on AGEs formation using biophysical techniques. *Sci Rep.* **2016**, *6*, 20414.
53. Ashraf, J. M.; Ansari, M. A.; Choi, I.; Khan, H. M.; Alzohairy, M. A. Antiglycating potential of gum arabic capped-silver nanoparticles. *Appl. Biochem. Biotechnol.* **2014**, *174*, 398-410.
54. Coussons, P. J.; Jacoby, J.; McKay, A.; Kelly, S. M.; Price, N. C.; Hunt, J. V. Glucose modification of human serum albumin: a structural study. *Free Radic. Biol. Med.* **1997**, *22*, 1217-1227.
55. Kousar, S.; Sheikh, M. A.; Asghar, M.; Sarwar, M. Effect of aminoguanidine on advanced glycation end products (AGEs) using normal and diabetic plasma. *J. Chem. Soc. Pak.* **2009**, *31*, 109-114.
56. Yu, S.; Zhang, W.; Liu, W.; Zhu, W.; Guo, R.; Wang, Y.; Zhang, D.; Wang, J. The inhibitory effect of selenium nanoparticles on protein glycation *in vitro*. *Nanotechnology* **2015**, *26*, 145703.
57. Ardestani, A.; Yazdanparast, R. Inhibitory effects of ethyl acetate extract of Teucrium polium on in vitro protein glycoxidation. *Food Chem. Toxicol.* **2007**, *45*, 2402-2411.
58. Hayase, F.; Shibuya, T.; Sato, J.; Yamamoto, M. Effects of oxygen and transition metals on the advanced Maillard reaction of proteins with glucose. *Biosci. Biotechnol. Biochem.* **1996**, *60*, 1820-1825.
59. Ortwerth, B. J.; James, H. Y.; Simpson, G.; Linetsky, M. The generation of superoxide anions in glycation reactions with sugars, osones, and 3-deoxyosones. *Biochem. Biophys. Res. Commun.* **1998**, *245*, 161-165.
60. Gillery, P.; Monboisse, J. C.; Maquart, F. X.; Borel, J. P. Glycation of proteins as a source of superoxide. *Diabete Metab.* **1987**, 14, 25-30.
61. Mullarkey, C. J.; Edelstein, D.; Brownlee, M. Free radical generation by early glycation products: a mechanism for accelerated atherogenesis in diabetes. *Biochem. Biophys. Res. Commun.* **1990**, *173*, 932-939.
62. Nakagawa, T.; Yokozawa, T.; Terasawa, K.; Shu, S.; Juneja, L. R. Protective activity of green tea against free radical- and glucose-mediated protein damage. *J. Agric. Food Chem.* **2002**, *50*, 2418-2422.
63. Kim, H. Y.; Kim, K. Protein glycation inhibitory and antioxidative activities of some plant extracts in vitro. *J. Agric. Food Chem.* **2003**, *51*, 1586-1591.
64. Kim, H. Y.; Lee, J. M.; Yokozawa, T.; Sakata, K.; Lee, S. Protective activity of flavonoid and flavonoid glycosides against glucose-mediated protein damage. *Food Chem.* **2011**, *126*, 892-895.
65. Yamaguchi, F.; Ariga, T.; Yoshimura, Y.; Nakazawa, H. Antioxidative and anti-glycation activity of garcinol from Garcinia indica fruit rind. *J. Agric. Food Chem.* **2000**, *48*, 180-185